

Electrochemical and quantum chemical investigation of the Cu^I and Cu^{II} complexes with biquinolyl monomer and polymer ligands

T. V. Magdesieva,^{a*} A. V. Dolganov,^a P. M. Polestchuk,^a A. V. Yakimanskii,^b
M. Ya. Goikhman,^b I. V. Podeshvo,^b and V. V. Kudryavtsev^b

^aDepartment of Chemistry, M. V. Lomonosov Moscow State University,
1 Leninskie Gory, 119992 Moscow, Russian Federation.
E-mail: tvn@org.chem.msu.ru

^bInstitute of High-Molecular-Weight Compounds, Russian Academy of Sciences,
31 Bol'shoi prosp., 199004 St. Petersburg, Russian Federation

Structural reorganization of polyamide (PA) and low-molecular-weight Cu^I and Cu^{II} complexes with biquinolyl (biQ) ligands during their mutual redox transformations in solution was studied using the electrochemical methods (cyclic voltammetry and preparative electrolysis) and quantum chemical DFT calculations. The influence of electronic factors and geometry distortions in the complexes on the ionization energy on going from Cu^I to Cu^{II} was evaluated in comparison. The catalytically active form of the [Cu^I(PA)L₂]BF₄ complex can be synthesized *in situ* from the stable tetrahedral complex [Cu^I(PA)₂]BF₄ by the series of successive redox transitions Cu^I → Cu^{II} → Cu^I accompanied by the loss of one biQ-containing macroligand.

Key words: copper-containing polymers, biquinolyl complexes, quantum chemical DFT calculations, electrochemically oxidation and reduction.

The copper complexes with biquinolyl (biQ) ligands are widely used as catalysts, photosensitizers, photoluminescent materials, *etc.* due to their unique properties.^{1–4} Modification of the coordination sphere by the introduction of different substituents into the biQ fragment changes the electronic and steric properties of the ligand, which makes it possible to synthesize complexes with specified properties. An important distinctive feature of the Cu^{I/II} redox pair is the tendency of structural reorganization (change in the type of coordination polyhedron) accompanying the electron transfer. This is related to the fact that the Cu^{II} complexes are characterized by the square-planar ligand environment with the coordination number (CN) equal to 4, square pyramid or trigonal bipyramid with CN = 5, or octahedron with CN = 6.⁵ In the case of the Cu^I complexes, tetrahedron is a preferential polyhedron.⁵ Therefore, the introduction of the Cu^{I/II} redox pair into the system can form a basis for the creation of electrochemically triggered "molecular machine."^{6–9}

We have recently synthesized^{10,11} new Cu^I complexes with conformationally non-rigid ligands based on polyamido acids (PA) containing the biQ fragments in the main chain (Scheme 1).

Electrosynthesis was carried out in *N*-methylpyrrolidone (NMP) in an undivided cell using the soluble copper anode. If the concentration of the starting poly-

mer is >10^{−4} mol L^{−1}, the violet precipitate of the [Cu^I(PA)₂]BF₄ polymer is formed in which the Cu atom is coordinated to two biQ fragments of the polymer chain. When the electrosynthesis is carried out in dilute solutions, two types of coordination modes can be obtained depending on the experimental conditions (amount of generated Cu^I in solution): [Cu^I(PA)₂] or [Cu^I(PA)L₂] containing in the Cu coordination sphere two biQ fragments or one biQ fragment of the polymer chain and two solvent molecules (L).

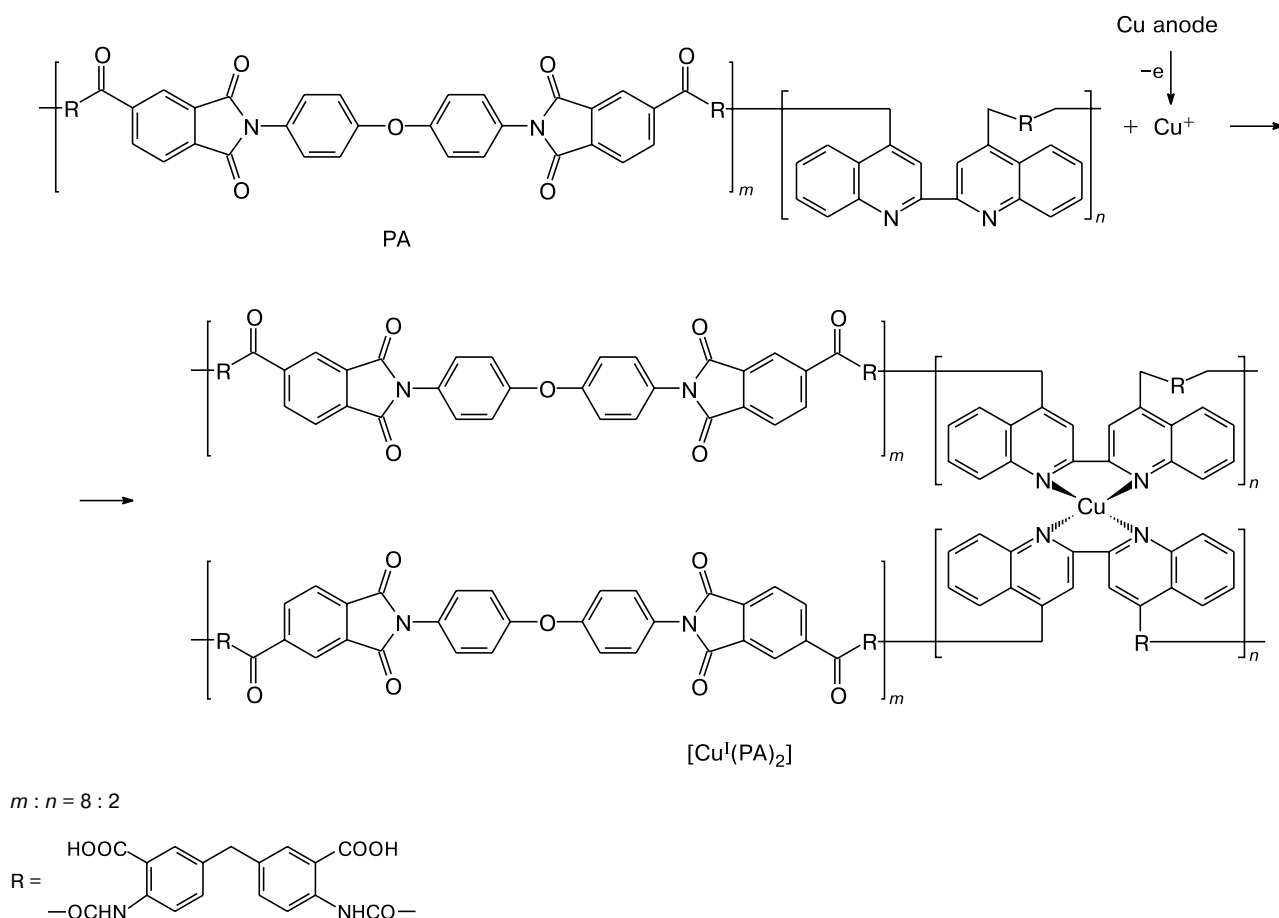
Since the synthesized Cu-polymer and especially its form [Cu^I(PA)L₂] manifest high catalytic activity in the reduction of O₂ and in oxygen activation in various oxidative processes,¹¹ it is of special interest to study mutual transitions of two forms of the complexes and structural reorganization accompanying the Cu^{I/II} redox transition.

The purpose of this work is to study routes of structural reorganization of the polymer and monomer Cu^I and Cu^{II} complexes with the biQ ligands during their mutual redox transitions in solution using electrochemical methods and quantum chemical calculations.

Experimental

N-Methylpyrrolidone (NMP) (bp 57 °C (5 Torr), *n*_D²⁰ = 1.4700) was purified by the treatment with calcium

Scheme 1



hydride and distilled under reduced pressure. Acetonitrile (pure grade) was stirred for 12 h over CaH_2 and distilled, then refluxed for 2 h over P_2O_5 , and distilled again, collecting the fraction with bp 81–82 °C (760 Torr).

Electrochemical oxidation and reduction potentials of the complexes were measured using an IPC_Win digital potentiostatic galvanostat attached to a computer. Voltammograms were detected in 0.05 M $\text{Bu}^n_4\text{NBF}_4$ in MeCN and NMP at 20 °C in a 8-mL electrochemical cell. Oxygen was removed from the cell by purging dry argon in the cell. Voltammetric curves were recorded by cyclic voltammetry (CV) at a stationary Pt electrode at different potential sweep rates. Electrolysis was carried out using a P-5827 M potentiostat in an electrochemical undivided cell 8 mL in volume. The working electrode was a Cu or Pt plate with a surface area of 0.6 and 0.4 cm^2 , respectively, and the auxiliary electrode was a Pt plate or special graphite (pyrolyzed polyacrylonitrile). In all experiments, the reference electrode was a saturated Ag/AgCl/KCl electrode (potential vs $\text{Fc}/\text{Fc}^+ = -0.48$ V). The measured potential values were recalculated taking into account ohmic losses.

Quantum chemical calculations were performed using the PRIRODA-04 program¹² on an MVS-6000IM computer cluster at the Joint Supercomputer Center of the Russian Academy of Sciences (Moscow) by the DFT method using the PBE non-local exchange functional.¹³ For all elements except hydrogen,

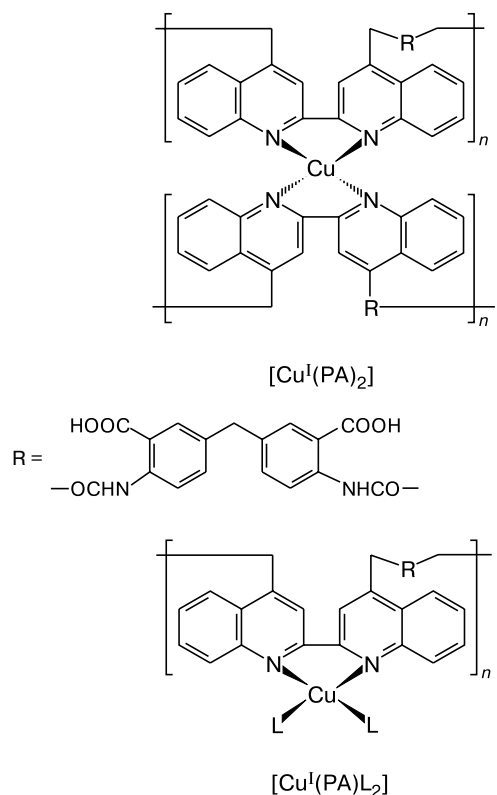
the core electronic shells were presented by the effective core SBK potential¹⁴ with the extended split TZ-2p basis set for valence electrons ((311/1) for H, (311/311/11) for C, N, and O, and (51111/51111/51111) for Cu).¹²

The structures under study were optimized without any structural restrictions imposed by the symmetry of molecules, *i.e.*, all calculations were performed in the framework of the point group symmetry C_1 .

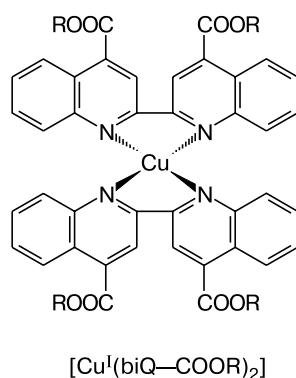
Results and Discussion

The Cu^{I} and Cu^{II} complexes with the polymer (PA) ligands and model low-molecular-weight biQ-containing complexes were chosen for the study.

This choice of the objects made it possible to study the influence of various factors on the oxidation potentials of the Cu^{I} and Cu^{II} complexes with the biQ ligands. For example, comparing the properties of the complexes with the polymer and model low-molecular-weight ligands, we managed to evaluate whether the conformation effect of the polymer chain on the electrochemical properties of the complexes is substantial or not. A comparison of the Cu^{I} and Cu^{II} complexes with the same ligands made it



L = NMP, MeCN



R = OC_6H_{13}

possible to reveal the effect of the charge factor on the properties of the complexes.

Quantum chemical methods make it possible to estimate the relative energy of complexes with different ligand environments in the gas phase, whereas the experimentally measured electrochemical oxidation and reduction potentials include the solvation energy, which partially "damps" the electronic effects and, to the contrary, increases the contribution of structural reorganization. Thus, quantum chemical and electrochemical considerations of the properties of the complexes supplement each other and allow one to describe most adequately the regularities observed.

Quantum chemical calculations. The calculations were performed by the density functional theory for a series of model structures containing the biQ ligands and (or) solvent molecules in the coordination sphere of Cu^{I} and Cu^{II} . The solvents were chosen to be MeCN and NMP in which electrosynthesis of the polymer complexes and their electrochemical investigation were carried out. For NMP we considered two possible coordination modes with the copper atoms: to the O atom ($_{\text{O}}\text{NMP}$) and to the N atom ($_{\text{N}}\text{NMP}$) (Fig. 1), because the affinity of the Cu^{I} and Cu^{II} atoms to these donor centers differs. The geometric parameters of the optimized structures for the complexes under study are given in Table 1. The data presented show that the transition from the Cu^{I} complexes to the systems with Cu^{II} is always accompanied by a decrease in the $\text{X}_1-\text{X}_2-\text{X}_3-\text{X}_4$ dihedral angle ($\text{X}_i = \text{N}, \text{O}$) (Fig. 2). This is due to the fact that the tetracoordinate Cu^{I} complexes are prone to form tetrahedral structures, and tetragonal configuration is more typical of the Cu^{II} complexes.¹⁵ In addition, the $\text{Cu}-\text{X}_i$ bond length shortens on going from Cu^{I} to Cu^{II} by $\sim 0.02-0.09$ Å. These data indicate an

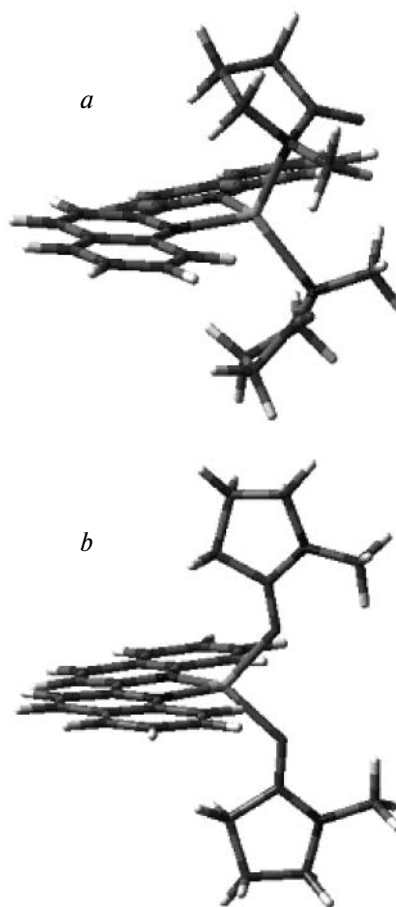


Fig. 1. DFT-calculated structures of the $[\text{Cu}^{\text{I}}(\text{biQ})(\text{NMP})_2]$ complexes in which the NMP molecules are coordinated to the Cu ion at the N (a) and O (b) atoms.

Table 1. DFT-calculated energy and geometric parameters of the Cu^I and Cu^{II} complexes with the monomer and polymer biQ-containing ligands

Compound	$-E_{\text{tot}}/\text{au}$	$-E_{\text{f}}/\text{kcal mol}^{-1}$ (eV) ^a	$E^{\text{rel } b}$	$E_{\text{i}}^{\text{ad } c}$	E_{i}^{v}	$-E_{\text{HOMO}}^d$	Geometric parameters ^e			
							eV	$d(\text{Cu}-\text{X}_i)/\text{\AA}$	α	β
									deg	
Cu ^I	196.14308	—	—	20.99	20.99	13.72	—	—	—	
Cu ^I (biQ)	325.53206	114.8 (4.98)	2.86	10.78	10.86	8.18	1.958	2.3	—	
Cu ^I (biQ) ₂	454.84334	180.9 (7.84)	0.00	8.95	9.23	7.31	2.021	0.2	89.0	
Cu ^I (_N NMP)(biQ)	385.29867	140.0 (6.07)	1.77	10.11	10.25	7.87	1.988, 2.089, 2.006 (_N NMP)	12.9	—	
Cu ^I (_N NMP) ₂ (biQ)	445.02840	142.1 (6.16)	1.68	9.67	9.79	7.49	2.067, 2.236 (_N NMP)	13.8	71.0	
Cu ^I (_O NMP)(biQ)	385.32291	155.2 (6.73)	1.11	9.45	9.62	7.02	1.993, 2.048, 1.908 (_O NMP)	7.6	—	
Cu ^I (_O NMP) ₂ (biQ)	445.07198	169.4 (7.35)	0.49	8.62	8.81	6.45	2.030, 2.040 (_O NMP)	4.8	83.5	
Cu ^I (MeCN)(biQ)	348.65929	158.9 (6.89)	0.95	10.14	10.24	7.85	2.023, 1.833 (MeCN)	0.6	—	
Cu ^I (MeCN) ₂ (biQ)	371.74017	173.9 (7.54)	0.30	9.54	9.73	7.36	2.064, 1.932 (MeCN)	3.4	82.7	
Cu ^{II}	195.37162	—	—	—	—	—	—	—	—	
Cu ^{II} (biQ)	325.13574	350.2 (15.19)	4.69	—	—	—	1.940	14.7	—	
Cu ^{II} (biQ) ₂	454.51440	458.6 (19.88)	0.00	—	—	—	2.007	5.8	60.3	
Cu ^{II} (_N NMP)(biQ)	384.92719	391.0 (16.95)	2.93	—	—	—	1.953, 2.012, 2.025 (_N NMP)	8.5	—	
Cu ^{II} (_N NMP) ₂ (biQ)	444.67301	403.2 (17.48)	2.40	—	—	—	2.027, 2.239 (_N NMP)	3.8	63.6	
Cu ^{II} (_O NMP)(biQ)	384.97570	421.5 (18.27)	1.61	—	—	—	1.942, 1.954, 1.865 (_O NMP)	0.4	—	
Cu ^{II} (_O NMP) ₂ (biQ)	444.75533	454.8 (19.72)	0.16	—	—	—	1.983, 1.987 (_O NMP)	2.6	55.2	
Cu ^{II} (MeCN)(biQ)	348.28673	409.2 (17.74)	2.14	—	—	—	1.971, 1.891 (MeCN)	0.3	—	
Cu ^{II} (MeCN) ₂ (biQ)	371.38955	438.0 (18.99)	0.89	—	—	—	1.991, 1.985 (MeCN)	4.4	59.0	

^a The total electronic energies for biQ, NMP, and MeCN are -129.20597 , -59.72647 , and -23.05699 au, respectively.

^b The relative energies of formation are $E^{\text{rel}} = E_f^{\text{compl}} - E_f(\text{Cu}(\text{biQ})_2^{I/II})$, compl is complex.

^c E_i^{ad} and E_i^v are the adiabatic and vertical ionization energies. For comparison, the experimental ionization energy of the Cu^I cation is 20.29 eV.

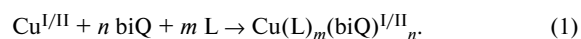
^d Energy of the higher occupied MO (HOMO).

^e Geometric parameters of the molecular systems: $d(\text{Cu}-\text{X}_i)$ is the distance between the Cu atom and X_i ($\text{X}_i = \text{N}, \text{O}$), α are torsion angles between two quinolyl systems, *i.e.*, $\text{N}-\text{C}-\text{C}-\text{N}$; β are torsion angles for four heteroatoms, which are directly bonded with the Cu atom, $\text{X}_1-\text{X}_2-\text{X}_3-\text{X}_4$ ($\text{X} = \text{N}, \text{O}$).

enhanced affinity of Cu^{II} to interaction with donor ligands, first of all, due to the high positive charge of copper. As for the turn of the quinoline rings about the C—C bridge in the biQ ligand, absolutely in all structures the N—C—C—N dihedral angle is substantially smaller than that in the free ligand (34.2°); in the most cases, its value comprises only units of degrees. Such small values of the dihedral angles indicate a very high binding energy of copper with biquinolyl.

For quantitative characterization of the ability of copper to bind with the ligands studied in the work, we calcu-

lated the energies of formation (E_f) of the complexes in the gas phase, *i.e.*, energies of the process



The data in Table 1 show that the most stable complex is formed by the Cu^I and Cu^{II} atoms with two biQ molecules. For instance, for Cu^I the E_f value is $-180.9 \text{ kcal mol}^{-1}$, which is more than twofold lower than that in the case of Cu^{II} ($-458.6 \text{ kcal mol}^{-1}$). This is completely consistent with the above indicated tendency

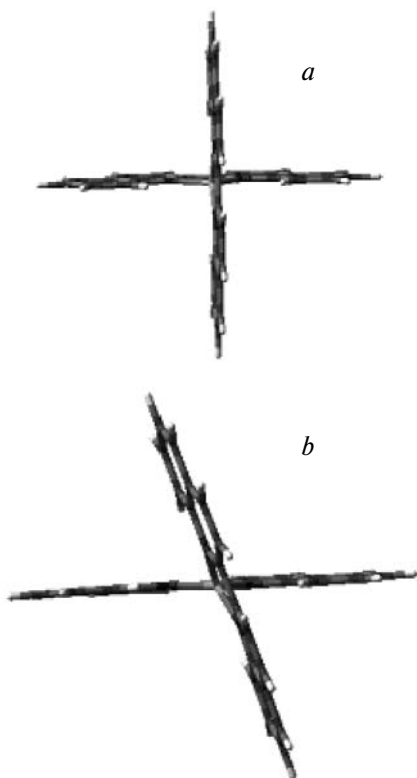


Fig. 2. DFT-calculated structures of the $[\text{Cu}^{\text{I}}(\text{biQ})_2]$ (a) and $[\text{Cu}^{\text{II}}(\text{biQ})_2]$ (b) complexes.

for copper–ligand bond shortening. It should be mentioned that for Cu^{II} the energies of formation of the $\text{Cu}^{\text{II}}(\text{biQ})_2$ and $\text{Cu}^{\text{II}}(\text{ONMP})_2(\text{biQ})$ complexes are almost the same (see Table 1, *cf.* -458.6 and $-454.8 \text{ kcal mol}^{-1}$).

For convenience of comparison of the relative stability of the compounds under study, we introduced the relative energies of formation E_{rel} , which are presented in Table 1. Analyzing these values, we can conclude that the stability of the Cu^{I} complexes decreases in the series $\text{Cu}^{\text{I}}(\text{biQ})_2 > \text{Cu}^{\text{I}}(\text{MeCN})_2(\text{biQ}) > \text{Cu}^{\text{I}}(\text{ONMP})_2(\text{biQ}) > \text{Cu}^{\text{I}}(\text{MeCN})(\text{biQ}) > \text{Cu}^{\text{I}}(\text{ONMP})(\text{biQ}) > \text{Cu}^{\text{I}}(\text{NMP})_2(\text{biQ}) > \text{Cu}^{\text{I}}(\text{NMP})(\text{biQ}) > \text{Cu}^{\text{I}}(\text{biQ})$, and that of the Cu^{II} complexes decreases in the order $\text{Cu}^{\text{II}}(\text{biQ})_2 > \text{Cu}^{\text{II}}(\text{ONMP})_2(\text{biQ}) > \text{Cu}^{\text{II}}(\text{MeCN})_2(\text{biQ}) > \text{Cu}^{\text{II}}(\text{ONMP})(\text{biQ}) > \text{Cu}^{\text{II}}(\text{MeCN})(\text{biQ}) > \text{Cu}^{\text{II}}(\text{NMP})_2(\text{biQ}) > \text{Cu}^{\text{II}}(\text{NMP})(\text{biQ}) > \text{Cu}^{\text{II}}(\text{biQ})$.

The second place by stability among the Cu^{I} complexes is occupied by $\text{Cu}^{\text{I}}(\text{MeCN})_2(\text{biQ})$ comprising two MeCN molecules ($E_{\text{rel}} = 0.30 \text{ eV}$). Among the Cu^{II} complexes, an analogous complex occupies the third place ($E_{\text{rel}} = 0.89 \text{ eV}$), whereas the second in stability is the Cu^{II} complex with NMP in which the Cu atom is bound to the O atom: $\text{Cu}^{\text{II}}(\text{ONMP})_2(\text{biQ})$ ($E_{\text{rel}} = 0.16 \text{ eV}$). This is primarily related to the very high affinity of Cu^{II} to oxygen, which is most pronounced when comparing the E_{rel} values for the copper complexes with ONMP and NMP. For

instance, for this type of complexes the difference in E_{rel} is equal to 1.19 eV (for Cu^{I}) and 2.24 eV (from Cu^{II}).

From the viewpoint of this work, the most interesting and important magnitudes are the ionization energies (E_i) of the complexes (see Table 1).

The ionization energy should be distinguished as adiabatic and vertical energies; the latter includes no energy of structural relaxation of the Cu^{II} complex. In this work, we calculated the both sets of values to evaluate how strongly the distortion of the geometry of the complex influences on E_i on going from Cu^{I} to Cu^{II} (so-called "geometric factor"). As can be seen from the data in Table 1 and Fig. 1, geometry distortion exerts no basic effect on the E_i values, *i.e.*, no changes occur in the relative arrangement in the series of ionization energies for the Cu^{I} and Cu^{II} complexes. This is shown in Fig. 3 as the fact that the E_i^{ad} and E_i^{v} values in the series of the studied complexes change in parallel.

The most easily ionized compound is $\text{Cu}^{\text{I}}(\text{ONMP})_2(\text{biQ})$, which is associated with the very high stabilization energy of the $\text{Cu}^{\text{II}}(\text{ONMP})_2(\text{biQ})$ complex formed upon ionization due to the presence of the Cu–O bond. Thus, the main reason for the low E_i value of the $\text{Cu}^{\text{I}}(\text{ONMP})_2(\text{biQ})$ complex as compared to $\text{Cu}^{\text{I}}(\text{biQ})_2$ and other complexes in the gas phase are the electronic effects of Cu^{I} cation stabilization by the O atoms rather than geometry distortions leading to oxidation product destabilization. However, the calculated data were obtained only for the gas phase, whereas in solution the solvation energy can substantially decrease the contribution of electronic effects, thus increasing the specific weight of the geometric factor.

In addition to the complexes with $L = \text{MeCN}$ ($n = 1, m = 1$ and 2) listed in Table 1, we also calculated the system with $m = 3$ (Fig. 4). This complex is not formed

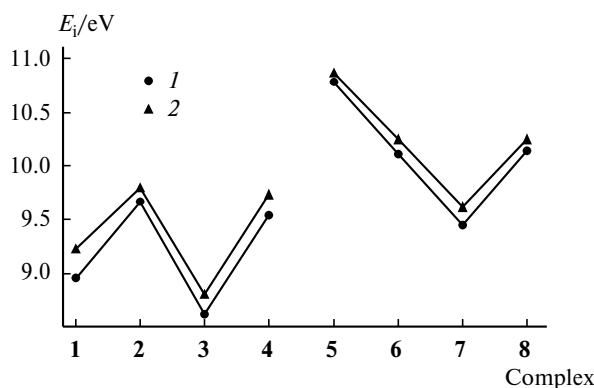


Fig. 3. Plots of the adiabatic (1) and vertical (2) ionization energies vs type of the complex ion: $[\text{Cu}^{\text{I}}(\text{biQ})_2]$ (1), $[\text{Cu}^{\text{I}}(\text{NMP})_2(\text{biQ})]$ (2), $[\text{Cu}^{\text{I}}(\text{ONMP})_2(\text{biQ})]$ (3), $[\text{Cu}^{\text{I}}(\text{MeCN})_2(\text{biQ})]$ (4), $[\text{Cu}^{\text{I}}(\text{biQ})]$ (5), $[\text{Cu}^{\text{I}}(\text{NMP})_2(\text{biQ})]$ (6), $[\text{Cu}^{\text{I}}(\text{ONMP})(\text{biQ})]$ (7), and $[\text{Cu}^{\text{I}}(\text{MeCN})(\text{biQ})]$ (8).



Fig. 4. DFT-calculated structure of $[\text{Cu}^{\text{II}}(\text{biQ})(\text{MeCN})_3]$ complex.

with Cu^{I} , because the third MeCN molecule is not bound with the Cu atom and, as a result, the $\text{Cu}^{\text{I}}(\text{MeCN})_2(\text{biQ})$ complex and the MeCN molecule remote from it are formed, whose interaction energy is only $2.5 \text{ kcal mol}^{-1}$. In the case of Cu^{II} , one managed to calculate the complex in which the Cu—MeCN distances are short enough (2.167, 2.040, 2.040 Å) to speak about the certain complex ion. The data in Table 1 indicate a tendency for decreasing E_i upon the introduction of many MeCN molecules. Indeed, at $m = 3$ the E_i^{ad} value of the separated $[\text{Cu}^{\text{I}}(\text{MeCN})_2(\text{biQ})] \dots \text{MeCN}$ system is 8.92 eV, which is very close to an analogous value for $\text{Cu}^{\text{I}}(\text{biQ})_2$ ($E_i^{\text{ad}} = 8.95 \text{ eV}$). It should be expected that the increase in the number of MeCN molecules surrounding the $\text{Cu}^{\text{II}}(\text{MeCN})_3(\text{biQ})$ complex can result, in the ultimate case, in a considerable decrease in E_i for the $\text{Cu}^{\text{II}}(\text{MeCN})_2(\text{biQ})$ complex. The same concerns the $\text{Cu}^{\text{II}}(\text{ONMP})_m(\text{biQ})$ complexes.

The series of the systems under study shows no ambiguous correspondence between the HOMO energies of Kohn—Sham orbitals and E_i values predicted by the Koopmans theorem. Although in the first approximation the higher is the HOMO energy, the lower is the ionization energy, conclusions about the ability of the complex ion to be ionized should be drawn carefully if these assumptions are based only on the data on E_{HOMO} , which is clearly demonstrated in Fig. 5.

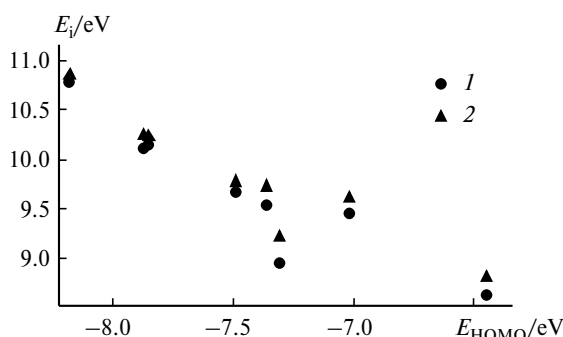


Fig. 5. Relation between the adiabatic (1) and vertical (2) ionization energies and the HOMO energy value.



Fig. 6. DFT-calculated structure of the Cu^{I} complex with NMP and two biQ ligands ($\text{Cu}^{\text{I}}(\text{ONMP})(\text{biQ})_2$) in which one of the biQ ligands is bonded to the Cu^{I} atom through only one N atom.

In addition to the systems described, we studied the copper complex with the NMP molecule and two biQ ligands, one of which is bound to the Cu atom only through one N atom (Fig. 6). This system makes it possible to estimate the E_i value when the additional polymer chain linked with biquinoyl prevents free rotation of the quinoyl rings about the C—C bond. In this case, one of the N atoms of biQ cannot be added to the Cu atom and, as a result, the Cu atom coordinates one NMP ligand instead.

Since the stability of the biQ complex with Cu^{I} and Cu^{II} is higher than that in the case of $\text{Cu}^{\text{I/II}}(\text{ONMP})_2(\text{biQ})$ (for the E_{rel} values, see Table 1), it should be expected that the procedure of geometry optimization will not give the desirable result, because the energy of the optimized system is still higher than that for particular $\text{Cu}^{\text{I}}(\text{biQ})_2$ and NMP species. In fact, the required structures can be optimized for neither Cu^{I} , nor Cu^{II} . Therefore, the geometry was optimized with allowance for fixation of the N—C—C—N dihedral angle (α) = 90° for one of the biQ ligands.

The energies of formation E_f found for the optimized $\text{Cu}^{\text{I}}(\text{ONMP})(\text{biQ})_2$ and $\text{Cu}^{\text{II}}(\text{ONMP})(\text{biQ})_2$ structures were -172.3 and $-457.6 \text{ kcal mol}^{-1}$, and $E_{\text{rel}} = 0.37$ and 0.04 eV , respectively. This completely confirms the above assumptions on the relative stability of these complexes compared to $\text{Cu}^{\text{I/II}}(\text{biQ})_2$. Almost equal formation energies for $\text{Cu}^{\text{II}}(\text{ONMP})(\text{biQ})_2$ and for $\text{Cu}^{\text{II}}(\text{biQ})_2$ complexes indicate that the ability of the O atom in the NMP molecule to electronic stabilization of the Cu^{II} ion is compared with that for the N atom in the chelating biQ ligand. In the case of the Cu^{I} complex, stabilizing ability of the O atom is much lower than that of the N atom and, as

Table 2. Potentials (V) of the oxidation (E^{ox}) and reduction (E^{red}) peaks of the copper biquinolyl complexes (Pt, NMP, 0.05 M Bu₄NBF₄, 100 mV s⁻¹, vs Ag/AgCl/KCl)

Complex	Oxidation			Reduction		
	E^{ox}	E^{red}	$I^{\text{red}}/I^{\text{ox}}$	$-E^{\text{red}}$	$-E^{\text{ox}}$	$I^{\text{ox}}/I^{\text{red}}$
[Cu ^I (PA) ₂] ₂ BF ₄	0.68	0.36	0.91	1.05, 1.30, 1.62	— — —	— — —
[Cu ^I (PA)(NMP) ₂] ₂ BF ₄	0.37	0.32	0.35	1.05, 1.34, 1.65	— — —	— — —
PA	—	—	—	1.00, 1.27, 1.51	— 1.17 —	— 0.55 —
[Cu ^I (biQ—COOR) ₂] ₂ BF ₄	0.75	0.36	0.92	0.91, 1.24, 1.62	— 1.15 —	— 0.55 —
biQ—COOR	—	—	—	0.86, 1.34, 1.51	— 1.24 —	— 0.48 —
[Cu ^{II} (PA)(NMP) ₂] ₂ [BF ₄] ₂	0.87	0.30	0.51	0.55, 1.18, 1.65	— — —	— — —
[Cu ^{II} (biQ—COOR) ₂] ₂ [BF ₄] ₂	1.76*	1.05	0.31	1.15, 1.35, 1.55	— 1.24 —	— 0.85 0.85

* Measured in MeCN, because these data cannot be obtained in NMP due to the narrow oxidation potentials window.

a consequence, the Cu^I(biQ)₂ complex ion is considerably destabilized upon the cleavage of one Cu^I—N bond and formation of the Cu^I—O bond (by 0.37 eV). The calculated energy of the adiabatic ionization process E_i^{ad} of the Cu^I(_ONMP)(biQ)₂ complex is the same as that for Cu^I(_ONMP)(biQ), namely, 8.62 eV.

Electrochemical properties of the complexes. The electrochemical potentials of the oxidation and reduction peaks of the Cu^I and Cu^{II} complexes with the biQ-containing ligands are presented in Table 2. Measurements were carried out in NMP or MeCN at the Pt electrode with a sweep rate of 100 mV s⁻¹.

The complexes with the polymer ligands are of special interest. The [Cu^I(PA)₂]₂BF₄ complex is oxidized (Fig. 7, *a*) at low anodic potential (0.68 V), which is characteristic of the tetrahedral Cu^I complexes and agrees with the data of quantum chemical calculations. In the reverse scan, the re-reduction peak is observed (ratio $I^{\text{red}}/I^{\text{ox}} = 0.91$, indicating the stability of the Cu^{II} complex formed). As can be seen from the data in Fig. 7, *a*, the difference in the potentials of the forward and reverse peaks is rather high (320 mV). This indicates that the electron transfer is followed by the chemical step or structural reorganization of the complexes.¹⁶ The results of quantum chemical calculations indicate a considerable change in the dihedral angle on going from Cu^I(biQ)₂ to

Cu^{II}(biQ)₂ (89 and 60.3°, respectively). This is not surprising, because Cu^I and Cu^{II} are characterized, as a rule, by different coordination environment. In addition to the change in the type of coordination polyhedron, the change in the dentate character of the ligand and partial replacement of the ligands by solvent molecules are possible, which should increase the difference in potentials of the forward and reverse peaks.

The [Cu^I(PA)(NMP)₂]₂BF₄ complex is oxidized at less anodic potential (Fig. 7, *b*) than its bisbiquinolyl analog [Cu^I(PA)₂]₂BF₄ (see Table 2), which agrees completely with data of quantum chemical calculations. As shown above, two reasons for this phenomenon are possible: high affinity of the Cu^{II} atom to the oxygen atom of NMP and a stronger deviation of the O—O—N—N dihedral angle from tetrahedral (55.2°, see Table 1). Two reduction peaks are detected in the reverse scan: at potentials 0.32 ($I^{\text{red}}/I^{\text{ox}} = 0.35$, $\Delta E = 50$ mV) and -0.55 V. This indicates that the electrochemical step is followed by a chemical reaction, for example, coordination to one more solvent molecule.

To reveal conformational effects on the potential of the Cu^{I/II} redox coupling, we studied the electrochemical oxidation of the model [Cu^I(biQ—COOR)₂]₂BF₄ complex with low-molecular-weight ligand. As can be seen from the data in Table 2, $E^{\text{ox}} = 0.75$ V, *i.e.*, the oxidation

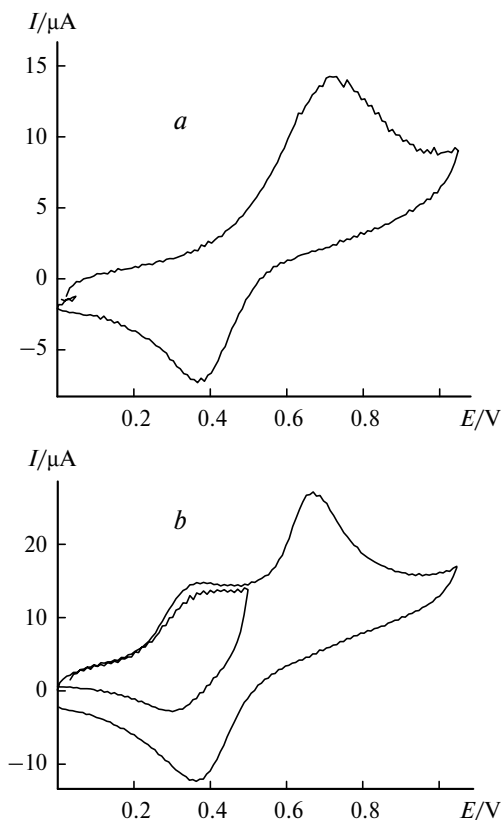


Fig. 7. CV curves for the complexes synthesized by electrolysis: $[\text{Cu}^{\text{I}}(\text{PA})_2]\text{BF}_4$ (a) and a mixture of $[\text{Cu}^{\text{I}}(\text{PA})\text{L}_2]\text{BF}_4$ and $[\text{Cu}^{\text{I}}(\text{PA})_2]\text{BF}_4$ (b) (Pt, NMP, 0.05 M Bu_4NBF_4 , 100 mV s⁻¹, vs Ag/AgCl/KCl).

potentials of the polymeric and low-molecular-weight complexes differ slightly and the geometry of the both complexes is close to tetrahedral. However, in the case of the model complex, we failed to synthesize a complex with one biQ ligand, *viz.*, $[\text{Cu}^{\text{I}}(\text{biQ}-\text{COOR})\text{L}_2]\text{BF}_4$, even in Cu^{I} excess in solution. This is quite reasonable taking into account the data of quantum chemical calculations, because the energy of formation of the $[\text{Cu}^{\text{I}}(\text{biQ})_2]\text{BF}_4$ complex is substantially higher than that for $[\text{Cu}^{\text{I}}(\text{biQ})\text{L}_2]\text{BF}_4$ (see Table 1). Therefore, the polymer chain in the biQ ligand prevents the formation of the Cu^{II} complex with two biQ ligands due to conformational hindrance. Perhaps, some destabilization of the complex due to the change in the electronic properties of the ligand (substitution of biQ for solvent molecules, *e.g.*, NMP) is compensated by a decrease in the energy of the complex due to a decrease in steric repulsion of the bulky polymeric ligands (or fragments of the polymer chain).

Based on the CV curve (see Fig. 7, a), we can assume that the structural reorganization that occurs upon the oxidation of the $[\text{Cu}^{\text{I}}(\text{PA})_2]\text{BF}_4$ tetrahedral complex is the elimination of one biQ ligand and formation of the complex in which the Cu atom is coordinated to only one biQ fragment of the polymer chain and two solvent mol-

ecules, or the polymer chain is turned in such a way that the second biQ fragment becomes the monodentate ligand and the remaining coordination site is occupied by one solvent molecule (see Fig. 6). This is indicated by close values of the potentials of the re-reduction peaks observed at the reverse scan after passing the peaks with $E^{\text{ox}} = 0.37$ and 0.68 V. In addition, the data of quantum chemical calculations show (see above) that the ability of the O atom in the NMP molecule to stabilize the Cu^{II} ion is comparable with that for the N atom in the biQ ligand. In this case, the steric hindrance of the complex should decrease, because the polymer chain receives an additional degree of freedom.

Dynamic equilibrium between the Cu^{I} and Cu^{II} coordination complexes with one or two sterically hindered (2,9-dimethyl-1,10-phenanthroline (DMP)) ligands was studied.¹⁷ The difference in potentials of the $\text{Cu}^{\text{II/I}}$ redox transitions for two types of the complexes, *viz.*, $[\text{Cu}^{\text{I}}(\text{DMP})_2]$ and $[\text{Cu}^{\text{II}}(\text{DMP})\text{L}_2]$, is ~0.3 V, as in our case.

To reveal the nature of chemical transformations that occur upon the $\text{Cu}^{\text{I/II}}$ redox transition, the tetrahedral $[\text{Cu}^{\text{I}}(\text{PA})_2]\text{BF}_4$ complex was subjected to preparative electrochemical oxidation at a potential of +0.68 V. The initial violet solution turned yellow. The CV study of the obtained solution showed the oxidation peak at 0.87 V (Fig. 8, a), and the re-reduction peak at a potential of 0.30 V was detected at the reverse scan. When scanning in the cathodic region, the peak at a potential of -0.55 V can be observed, after which the oxidation peak at +0.38 V corresponding to $[\text{Cu}^{\text{I}}(\text{PA})\text{L}_2]\text{BF}_4$ (see above) appears in the reverse scan. The data obtained indicate that the oxidation of the $[\text{Cu}^{\text{I}}(\text{PA})_2]\text{BF}_4$ tetrahedral complex is accompanied by the elimination of one biQ ligand and additional coordination to solvent molecules, resulting in the formation of the catalytically active complex $[\text{Cu}^{\text{II}}(\text{PA})\text{L}_2]\text{BF}_4$. Preparative electrolysis at a potential of -0.55 V gives a violet solution again; however, its CV curve (Fig. 8, b) differs from that observed for the starting tetrahedral complex (see Fig. 7, a). A new peak appears at the potential of 0.38 V, confirming $[\text{Cu}^{\text{I}}(\text{PA})\text{L}_2]\text{BF}_4$ complex formation in the solution.

If the same electrochemical cycle ($\text{Cu}^{\text{I}} \rightarrow \text{Cu}^{\text{II}} \rightarrow \text{Cu}^{\text{I}}$) is carried out for the low-molecular-weight model complex $[\text{Cu}^{\text{I}}(\text{biQ}-\text{COOR})_2]\text{BF}_4$, the CV curves of the initial and final solutions turned out to be identical, *i.e.*, the $\text{Cu}^{\text{I/II}}$ redox transition is completely reversible and, as a result, the electrochemical cycle affords the starting complex. The determined potential difference between the forward and reverse peak (390 mV) is related, most likely, to the change in the dihedral angle (see Table 1)¹⁶ or additional coordination of the solvent molecule, but no elimination of the biQ ligand occurs.

The observed regularities can be described in the framework of Schemes 2 and 3.

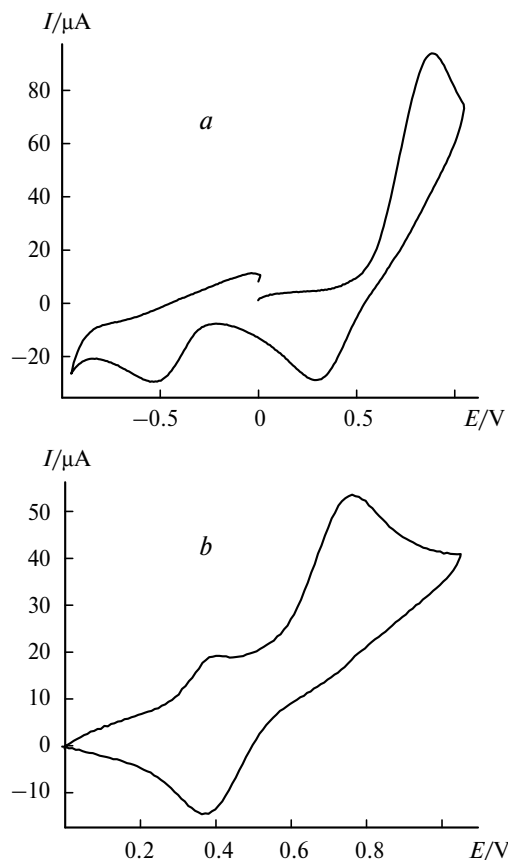
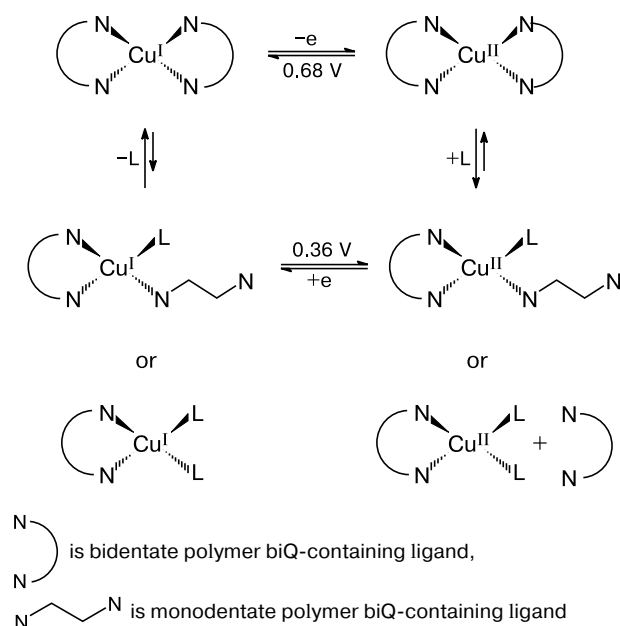


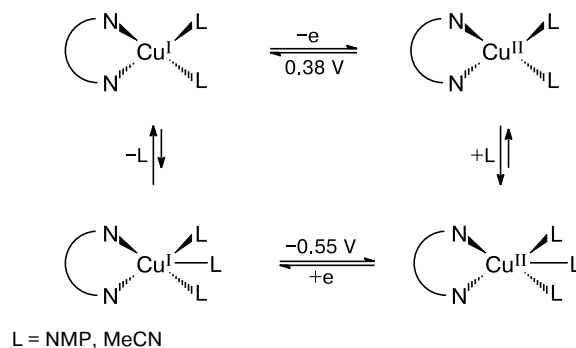
Fig. 8. CV curves of $[\text{Cu}^{\text{II}}(\text{PA})\text{L}_2][\text{BF}_4]_2$ (a) and a mixture of $[\text{Cu}^{\text{I}}(\text{PA})\text{L}_2]\text{BF}_4$ and $[\text{Cu}^{\text{I}}(\text{PA})_2]\text{BF}_4$ (b) obtained by potentiostatic electrolysis $\text{Cu}^{\text{I}} \xrightarrow{0.68 \text{ V}} \text{Cu}^{\text{II}} \xrightarrow{-0.55 \text{ V}} \text{Cu}^{\text{I}}$ (Pt, NMP, 0.05 M Bu_4NBF_4 , 100 mV s^{-1} , vs Ag/AgCl/KCl).

According to the presented scheme, the $\text{Cu}^{\text{I/II}}$ redox transition is accompanied by reversible changes in the coordination sphere of the Cu ions. Since the data of quantum chemical calculations showed that the NMR molecule and biQ ligand are approximately equivalent in electronic stabilization of the Cu^{II} ion, the driving force of ligand exchange presented in Scheme 2 is the decrease in steric repulsion in the Cu^{II} complex, which appears upon a change in the dihedral angle in the coordination polyhedron, because the square-planar ligand environment is preferential for the Cu^{II} atoms. Examples for similar ligand exchange are known. For instance, it has been shown recently¹⁸ that when the solution contains two types of bipyridine ligands, one of which comprises bulky substituents, the electrochemically induced ligand exchange is observed at a potential of the $\text{Cu}^{\text{I/II}}$ redox transition. As a result, the solution contains the tetrahedral Cu^{I} complex with sterically hindered ligands and its oxidation is accompanied by the fast ligand exchange to form the square-planar Cu^{II} complex with the unsubstituted bipyridine ligands.

Scheme 2



Scheme 3



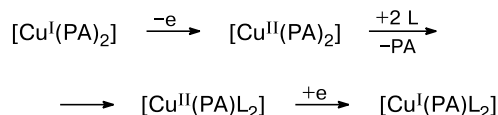
Scheme 3 shows the additional coordination of the third solvent molecule after Cu^{II} complex formation, which is accompanied by a change in the geometry. According to the data of quantum chemical calculations, the presence of the third donating sterically unhindered ligand stabilizes the complex.

Thus, the routes of structural reorganization of the polymeric and low-molecular-weight model Cu^{I} and Cu^{II} complexes with the biQ ligands that occur during their mutual redox transitions in solution were studied using the electrochemical methods and quantum chemical DFT calculations. The influence of the electronic factors and geometry distortion on the ionization energy on going from Cu^{I} to Cu^{II} was comparatively evaluated.

The results of electrochemical investigation of the $\text{Cu}^{\text{I/II}}$ redox transitions in the biQ-containing polymer

and model low-molecular-weight complexes indicate that the $[\text{Cu}^{\text{II}}(\text{PA})_2][\text{BF}_4]_2$ complex with two polymer ligands, unlike the starting $[\text{Cu}^{\text{I}}(\text{PA})_2]\text{BF}_4$ complex, is unstable because of steric interactions and easily eliminates one biQ ligand, and the liberated coordination site is occupied by the solvent molecules. Thus formed $[\text{Cu}^{\text{II}}(\text{PA})\text{L}_2][\text{BF}_4]_2$ complex can be reduced at a potential of -0.55 V to the Cu^{I} complex of the same composition. This complex is very reactive toward dioxygen and can serve as a catalyst of various oxidation processes involving activated dioxygen.¹¹ It is convenient to involve the obtained complex into the electrocatalytic process *in situ*. For this purpose, the $[\text{Cu}^{\text{I}}(\text{PA})_2]\text{BF}_4$ tetrahedral complex stable in air can be oxidized potentiostatically (at a potential of 0.68 V) with the loss of one biQ ligand to form $[\text{Cu}^{\text{II}}(\text{PA})\text{L}_2][\text{BF}_4]_2$, whose backward reduction affords the desired complex $[\text{Cu}^{\text{I}}(\text{PA})\text{L}_2]\text{BF}_4$. Thus, the electrochemical generation of the active form of the catalyst can be presented as Scheme 4.

Scheme 4



This work was supported by the Russian Foundation for Basic Research (Project No. 05-03-32759) and the St. Petersburg Scientific Center of the Russian Academy of Sciences.

References

1. E. K. van der Beuken and B. L. Feringa, *Tetrahedron*, 1998, **54**, 12985.
2. N. Wei, N. N. Murthy, Q. Chen, J. Zablata, and K. D. Karlin, *Inorg. Chem.*, 1994, **33**, 1953.
3. D. V. Scaltrito, D. W. Thompson, J. A. O'Callahan, and J. A. Mayer, *J. Coord. Chem. Rev.*, 2000, **208**, 243.
4. E. C. Riesgo, Y.-Z. Hu, F. Bouvier, R. P. Thummel, D. Scaltrito, and G. J. Mayer, *Inorg. Chem.*, 2001, **40**, 3413.
5. H. B. Gray, B. G. Malstrom, and R. J. P. Williams, *J. Biol. Inorg. Chem.*, 2000, **5**, 551.
6. M. H. Al-Sayah and N. R. Branda, *Chem. Commun.*, 2002, 178.
7. N. Armaroli, V. Balzani, J.-P. Collin, P. Gavina, J. P. Sauvage, and B. Ventura, *J. Am. Chem. Soc.*, 1999, **121**, 4397.
8. G. De Santis, L. Fabrizzi, D. Iacopino, P. Pallavicini, A. Perotti, and A. Poggi, *Inorg. Chem.*, 1997, **36**, 827.
9. A. Livoreil, C. O. Dietrich-Buchecker, and J. P. Sauvage, *J. Am. Chem. Soc.*, 1994, **116**, 9399.
10. M. Ya. Goikhman, I. V. Gofman, I. V. Podeshvo, E. L. Aleksandrova, A. O. Pozdnyakov, and V. V. Kudryavtsev, *Vysokomol. Soedin.*, 2003, **45A**, 1045 [*Russ. Polym. Sci.*, 2003, **45A** (Engl. Transl.)].
11. T. V. Magdesieva, A. V. Dolganov, A. V. Yakimanskii, M. Ya. Goikhman, I. V. Podeshvo, and V. V. Kudryavtsev, *Elektrokhimiya*, 2007, No. 9 [*Russ. J. Electrochem.*, 2007, No. 9 (Engl. Transl.)].
12. D. N. Laikov and Yu. A. Ustynyuk, *Izv. Akad. Nauk, Ser. Khim.*, 2005, 804 [*Russ. Chem. Bull., Int. Ed.*, 2005, **54**, 820].
13. J. P. Perdew, K. Burke, and M. Ernzerhof, *Phys. Rev. Lett.*, 1996, **77**, 3865.
14. W. J. Stevens, H. Basch, and M. Krauss, *J. Chem. Phys.*, 1984, **81**, 6026.
15. H. B. Gray, B. G. Malstrom, and R. J. P. Williams, *J. Biol. Inorg. Chem.*, 2000, **5**, 551.
16. K. Stolarczyk, R. Bilewicz, L. Siegfried, and T. Kaden, *Inorg. Chem. Acta*, 2003, **348**, 129.
17. Y. Lei and F. C. Anson, *Inorg. Chem.*, 1995, **14**, 1083.
18. S. Kume, M. Kurihara, and H. Nishihara, *Inorg. Chem.*, 2003, **42**, 2194.

Received December 26, 2006;
in revised form March 29, 2007